TITLE: *IN SITU* INFRARED STUDY OF CATALYTIC DECOMPOSITION OF NO

REPORT TYPE: Semiannual Technical Progress Report

REPORTING PERIOD: February 1, 1997 to August 1,1997

PRINCIPAL AUTHOR(s): Steven S.C. Chuang and Cher-Dip Tan

ISSUED REPORT DATE: July 17, 1997

INSTITUTION: The University of Akron
Department of Chemical Engineering
Akron, Ohio 44325-3906
(330) 972-6993

Disclaimer

Abstract

The growing concerns for the environment and increasingly stringent standards for NO emission have presented a major challenge to control NO emmissions from electric utility plants and automobiles. Catalytic decomposition of NO is the most attractive approach for the control of NO emission for its simplicity. Successful development of an effective catalyst for NO decomposition will greatly decrease the equipment and operation cost of NO control. Due to lack of understanding of the mechanism of NO decomposition, efforts on the search of an effective catalyst have been unsuccesful.

Scientific development of an effective catalyst requires fundamental understanding of the nature of active site, the rate-limiting step, and an approach to prolong the life of the catalyst. Research is proposed to study the reactivity of adsorbates for the direct NO decomposition and to investigate the feasibility of two novel approaches for improving catalyst activity and resistance to sintering. The first approach is the use of silanation to stabilize metal crystallites and supports for Cu-ZSM-5 and promoted Pt catalysts; the second is utilization of oxygen spillover and desorption to enhance NO decomposition activity. An innovative infrared reactor system will be used to observe and determine the dynamic behavior and the reactivity of adsorbates during NO decomposition, oxygen spillover, and silanation. A series of experiments including X-ray diffraction, temperature programmed desorption, temperature programmed reaction, X-ray photoelectron spectroscopy will be used to characterized the catalysts. The information obtained from this study will provide a scientific basis for developing an effective catalyst for the NO decomposition under practical flue gas conditions.

Table of Contents

List of Graphical Materials

Fig. 11 NO conversion as a function of temperature (light-off curves).

Executive Summary

During the *third* semi-annual period, two major tasks were accomplished.

(i)   The light-off characterestic of Rh/Al$_2$O$_3$ for NO-CO reaction was determined. Due to the presence of CO in the exhaust, and with use of Rh for NO abatement; it is important to determine the role of CO in the NO removal process on Rh before studying the effect of Tb-promotion.

(ii)   Results of this study show strong depenedence of the catalyst surface state on the reactant partial pressure.

Work is currently underway to determine the effect of H$_2$O on the catalyst activity and the transient behavior of adsorbates for NO decomposition and NO-CO reaction.

Light-off Characteristic of NO-CO Reaction over Rhodium Catalysts

Introduction

The major function of Rh in the three-way catalytic converter is to catalyze the reaction of NO with CO to form N_2 and CO_2 [1-10]. The NO or CO conversion for the NO-CO reaction over Rh catalyst is a function of temperature, reactant partial pressure, catalyst activity, flow pattern, and reactant residence time in the reactor. Steady-state conversion as a function of temperature for a specific flow reaction, shown in the bottom panel of Figure 1, has been used to characterize the light-off feature of a catalyst for CO-O_2 and NO-CO reactions [7-12]. The light-off characteristic provides a convenient way of evaluating the potential of a catalyst for commercial application.

Light-off temperature, at which 50% conversion is achieved under a specific flow condition, has been used as a measure of catalyst activity. An effective catalyst should achieve the light-off at low temperature. Above the light-off temperature, high conversion is achieved due to high reaction rates. Under this condition, the overall reaction process is often controlled by either external mass transfer or internal diffusion of the reactant into the catalyst pore [13]; the reaction process can be influenced by the severe heat effect due to high exothermicity of the NO-CO and CO-O_2 reactions. Below the light-off temperature, the reaction is the rate-controlling step; therefore, there are no diffusion limitations for the overall reaction process.

Since the Rh surface state is very sensitive to its chemical environment and reaction conditions, the significant difference in reaction conditions before and after light-

off may lead to different Rh surface states. In this paper, we employed Temperature-Programmed Reaction (TPR) coupled with Fourier Transform Infrared Spectroscopy (FTIR) to study the Rh surface states and their adsorbates as a function of reaction temperature, partial pressures, and Rh loadings. FTIR measured not only the adsorbate concentration but also temperature of the SiO_2 support with its overtone intensity. The effects of Rh loading, partial pressure of reactants, thermal effect, and feed rate on the light-off curve and the Rh surface state were determined to reveal the kinetic significance of the light-off curve.

Although the NO-CO reaction on Rh catalysts has been extensively studied [7-14], results of this study demonstrate the usefulness of TPR-IR for catalytic reaction studies, shed light into the NO-CO reaction mechansim, further reveal the interesting properties of the Rh surface, and unravel the light-off characteristic of the exothermic reactions.

Results

Figure 3 shows the IR spectra of adsorbates on 5 wt% Rh/SiO_2 catalyst during a TPR-IR study of NO-CO-He (10:50:30 cm^3/min). The effluent rate of products and the light-off curve corresponding to the infrared spectra are shown in Figure 4. Temperatures shown in Figures 3 and 4 were recorded from a thermocouple measuring the gas phase reaction temperature near the the catalyst pellet. An additional 1/16" thermocouple was placed at the exit of the IR cell to measure the effluent temperature. The temperature measured by both thermocouples was found to be the same for all the runs.

The mode of NO and CO adsorbates depends on Rh surface states which show strong temperature dependence. In the 303 - 413 K region, the low wavenumber $Rh-NO^-$ species at 1690 and 1627 cm^{-1} are the predominant adsorbates even at low NO/CO ratio. The presence of $Rh-NO^-$ indicates that the majority of the Rh surface remains in the reduced state; adsorbed NO is more strongly bonded than adsorbed CO on the reduced Rh surface. Although conversion of reactant is low in this temperature range, more NO

conversion than CO conversion was achieved with the formation of more N_2 than N_2O and CO_2, suggesting the occurrence of the following steps:

$$2NO \rightarrow N_2 + 2O_{ad} \qquad\qquad [2]$$

$$2NO \rightarrow N_2O + O_{ad}. \qquad\qquad [3]$$

The amount of O_{ad} reacted with adsorbed CO to produce CO_2 as shown by increasing IR intensity (Fig. 3) and effluent rate (Fig. 4) for CO_2 with temperature; some fraction of O_{ad} oxidized Rh^0 to Rh^+ resulting in the formation of $Rh^+(CO)_2$ at 2092 and 2035 cm^{-1}. This process may decrease the number of the reduce Rh^0 sites for Rh-NO$^-$ as demonstrated by decreasing Rh-NO$^-$ intensity with temperature.

The intensities of $Rh^+(CO)_2$ grew to their maximum at 523 K and then decreased. Infrared results in Fig. 3 and effluent rate results in Fig. 4 show that the rate of CO_2 formation began a marked increase at temperatures above 523 K. The intensity of Si-NCO at 2293 cm^{-1} which was identified as the spectator for CO_2 formation [13] increased to their maximum at 673 K.

The light-off temperature occurred near 580 K where gem-dicarbonyl, Rh-NCO, and Si-NCO were the major IR-observable adsorbates; N_2 and CO_2 were the major products. The temperature difference between the catalyst support (T_s) and gas phase (T_g) began to appear at temperatures above 500 K, as shown in Fig. 5. The temperature difference grew wider as conversion and temperature increased, revealing that the heat released from the reaction was accumulated on the catalyst pellet causing temperature rise of the SiO_2 support. The absence of temperature variation in the inlet and outlet of the reactor further unravels that the heat from the reaction was able to heat up the catalyst pellet, but was not enough to heat the reactant flow of 90 cm^3/min.

Results of the study with high partial pressure of NO-CO in Figs. 3 and 4 provide clear infrared spectra and mass spectrometer results for elucidation of reaction mechanism

and properties of Rh catalysts. However, these concentrations of NO and CO are significantly higher than those in the exhaust of automobile engines. Concentration of NO and CO was further reduced by 10 times for determining the effect of partial pressure of reactants on the Rh surface state and light-off characteristic. Figures 6 and 7 show the IR spectra of adsorbates and the rate of eluted products during the TPR-IR study of NO-CO-He (0.3:5:29.7 cm^3/min). Comparison of results in Figs. 3 and 6 shows that exposure of the catalyst to low reactant concentration led to the following observations: (i) the formation of linear CO at 2041 cm^{-1} with a red shift (decrease in the wavenumber) to 2017 cm^{-1} at 673 K, (ii) the lower light-off temperature at 473 K, and (iii) the absence of temperature difference between the support and reactant mixture (shown in Fig. 8).

Discussion

Reaction Mechanism

A number of the NO-CO reaction studies on Rh/SiO$_2$ catalysts have revealed that the reaction pathway for N$_2$ and CO$_2$ formation below light-off temperature is different from those above light-off [13,17]. Tables 2A and 2B list both reaction pathways. Above light-off, all the steps take place on the reduced Rh surface of supported Rh catalysts. These proposed steps listed in Table 2A are identical to those proposed for the reaction on Rh single crystal surfaces [5]. The Rh^0 site is the only type of site that has been reported on the Rh single crystal surface for the NO-CO reaction for the entire temperature range of reaction studies from 253 to 900 K, regardless of the light-off temperature.
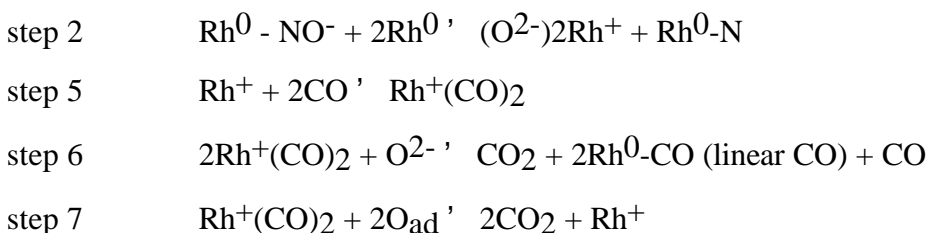
The difference in reaction pathway between supported Rh and Rh single crystal catalysts below light-off may result from the use of different reactant partial pressures. Results of this study show that the below light-off mechanism listed in Table 2B for supported Rh catalysts is only applicable to high partial pressures of NO and CO. Under such conditions, CO adsorbs on Rh$^+$ sites as Rh$^+$(CO)$_2$ and NO adsorbs as Rh-NO$^-$; the surface of supported Rh catalyst contains both Rh^0 and Rh$^+$ sites [13,17].

For the reaction under low partial pressure conditions, linear CO on the Rh^0 site is the dominant adsorbate at temperatures above 500 K (the light-off) whereas $Rh-NO^-$ is the major adsorbate below the light-off. These results are displayed in Fig. 6 and clearly show that no adsorbates associated with Rh^+ were observed for either above or below light-off. The surface of supported Rh catalysts consists of primarily the Rh^0 sites which have the same state as those on the Rh single crystal surface for catalyzing the NO-CO reaction. Most reaction studies on the Rh single crystal surface were carried out at CO and NO partial pressure below 40 Torr [5,18,19]. These NO and CO partial pressures are significantly below those for rapidly producing Rh^+ sites on Rh/SiO_2. It is unclear whether the use of high partial pressure NO for the reaction would convert Rh^0 to Rh^+ sites on the single crystal surface.

Figure 9 summarizes infrared spectra of adsorbates on the catalyst with various Rh loading under different partial pressures of reactants at 523 K. Rh loading has little effect on the nature of adsorbates, especially for $Rh^+(CO)_2$ formation. High loading Rh catalysts possess large reduced Rh crystallites while low loading Rh catalyst (i.e, 0.5 wt% Rh/SiO_2) has highly dispersed reduced Rh^0 sites prior to exposure to the NO-CO reactant mixture. Exposure of these reduced Rh crystallites to the NO-CO mixture at room temperature produced $Rh-NO^-$, indicating that the catalyst surface is in the reduced state. Increase in reaction temperature allows NO dissociation to occur. Oxygen from dissociated NO appears to induce oxidative disruption of the reduced Rh crystallite to isolated Rh^+ sites for CO adsorption as $Rh^+(CO)_2$. It has been shown that the oxidative disruption rate is significantly lower for large Rh crystallites than for small Rh crystallites [20-23]. The absence of particle size effects in the formation of $Rh^+(CO)_2$ may be attributed to the use of high NO partial pressure which rapidly oxidized Rh^0 to Rh^+ sites for both large and small Rh crystallites.

Dependence of $Rh^+(CO)_2$ Intensity on Rh Loadings, Temperature, and Reactant PartialPressures

Figure 10 shows the variation of $Rh^+(CO)_2$ intensity with temperature for Rh/SiO_2 under various Rh loading and reactant partial pressures. Since $Rh^+(CO)_2$ is associated with the Rh^+ site, the intensity of $Rh^+(CO)_2$ may represent the amount of Rh^+ sites. Consider the reaction steps 2, 5, 6, and 7 listed in Fig 2 B,

step 2 $\quad\quad Rh^0 - NO^- + 2Rh^0 \text{'} \quad (O^{2-})2Rh^+ + Rh^0\text{-}N$

step 5 $\quad\quad Rh^+ + 2CO \text{'} \quad Rh^+(CO)_2$

step 6 $\quad\quad 2Rh^+(CO)_2 + O^{2-} \text{'} \quad CO_2 + 2Rh^0\text{-}CO \text{ (linear CO)} + CO$

step 7 $\quad\quad Rh^+(CO)_2 + 2O_{ad} \text{'} \quad 2CO_2 + Rh^+$

These steps illustrate the processes for the formation and reduction of Rh^+ and $Rh^+(CO)_2$. Rh^+ sites for gem-dicarbonyl are generated from dissociation of adsorbed NO which oxidizes Rh^0 to Rh^+ sites (step 2). Rh^+ sites can be reduced by reductive agglomeration (step 6); $Rh^+(CO)_2$ can be consumed by reaction with O_{ad} to form CO_2 (step 7). Provided that steps 6 and 7 are slow steps for the catalytic process for CO_2 formation from CO, Rh^+ is saturated with gem-dicarbonyl. The increase in $Rh^+(CO)_2$ intensity with temperature from room temperature to 500K represents an increase in the number of Rh^+ sites. Temperature for maximum intensity (T_{max}) occurred at the point where the rate of increase for reductive agglomeration of Rh^+ and reaction of $Rh^+(CO)_2$ with O_{ad} with respect to temperature is greater that that for oxidative disruption of Rh^0 sites. Examination of the light-off curve in Figure 11 shows that T_{max} coincides with temperature where a marked increase in NO conversion occurs.

The relation between NO conversion, catalyst temperature, and $Rh^+(CO)_2$ intensity can be elucidated from the results of this study. High NO conversion released large amounts of heat and caused a significant increase in the temperature of SiO_2 and the Rh metal surface. This effect is manifested by a comparison of light-off curves and the SiO_2 temperature (shown in Figures 4/5 and 7/8). The Rh surface temperature should be higher than the SiO_2 temperature because the reaction takes place on the Rh surface where heat dissipates from Rh metal to the SiO_2 support. Therefore, rapid rise in the

light-off curve corresponds to the sharp increase in Rh surface temperature. High Rh surface temperature is known to favor the reductive agglomeration rather than the oxidative disruption [20-23]. Thus, the results of the sharp increase in the Rh surface temperature is a steep decrease in the $Rh^+(CO)_2$ intensity.

Qualitative Nature of the Light-off Curve

The light-off curve is a manifestation of the overall rates of the reaction process as a function of temperature. The overall rate of the reaction is influenced by the heat effect, mass transfer, reaction kinetics, and residence time of reactant. The mass transfer effect can be assessed from the slope of the light-off curve. For instance, the rate of reaction should increase exponentially with temperature. At temperatures above 630 K, the weak dependence of the rate and NO conversion on temperature (Figure 11) suggests that external mass transfer is the rate-limiting process; most NO reactant is consumed near the pellet surface.

The qualitative nature of the reaction kinetics may be elucidated from the dependence of the light-off curve. Comparison of the a and b curves shows that low partial pressure of NO decreases the light-off temperature, in other words, increases the reaction rate. The results confirm that the rate for the NO-CO reaction has negative order with respect to NO [24]. Comparison of the a and c curves shows that increasing the amount of the catalyst, corresponding to increasing the reactant residence time, caused a decrease in the light-off temperature.

Conclusion

Combined TPR-IR studies allow rapid scan of the intensity of various infrared-observable adsorbates and light-off characteristic as a function of temperature and reactant partial pressures. Combined TPR-IR studies over Rh/SiO_2 catalysts revealed the strong dependence of light-off characteristic and Rh surface state on the reactant partial pressure. Low NO (0.85KPa) and CO (16 KPa) partial pressures allow the Rh surface to

be maintained at the reduced state during the NO-CO reaction from room temperature to 673 K. High NO (0.01MPa) and CO (0.01MPa) partial pressures result in oxidation of Rh^0 to Rh^+ below the light-off. Temperatures above the light-off are required to reduce Rh^+ to Rh^0. The proposed mechanism for the NO-CO reaction from Rh single crystal studies is consistent with those for the reaction above light-off and low NO and CO partial pressures. Results of this study further confirm that the reduced Rh^+ site is more active than the Rh+ site for NO-CO reaction.

References

[1] J.T., Kummer, J. Phys. Chem. 90 (1986) 4747.

[2] K.C. Taylor, Catal. Rev. Sci. Eng. 35 (1993) 457.

[3] M. Shelef, and G.W. Graham, Catal. Rev. Sci. Eng. 36 (1994) 433.

[4] S.H. Oh, J. Catal. 124 (1990) 477.

[5] K.Y.S. Ng, D.N. Belton, S.J. Schmieg, and G.B. Fisher, J. Catal. 146 (1994) 396.

[6] R.W. McCabe, and C. Wong, J. Catal. 121 (1990) 422.

[7] B.K. Cho, J. Catal. 131 (1991) 74.

[8] S.H. Oh and J.C. Cavendish, A.I.Ch.E. J., 31 (1985) 935.

[9] S.S.C. Chuang, R. Krishnamurthy, and G. Srinivas, in U. Ozkan, S. Agarwal, and G. Marcelin (Editors), Symposium on NO_X Reduction, Series 587, American Chemical Society, Washington, DC, 1994, pp. 183.

[10] A.T Bell, and K.C. Taylor, in P. M., Eisenberger (Editor), Basic research Needs for Vehicles of the Future, Emission Control, Princeton Materials Institute, Princeton University, Princeton, New Jersey, 1995, pp. 33.

[11] G. Leclercq, C. Dathy, G. Mabilon, and L. Leclercq, in A. Crucq (Editor), Catalysis and Automotive Pollution Control II, Elsevier Science Publishers B.V., Amsterdam, 1991, pp 181.

[12] R. M. Heck and R. J. Farrauto, Catalytic Air Pollution Control: commercial Technology, Van Nostrand Reinhold, New York, 1995.

[13] R. Krishnamurthy, S.S.C. Chuang and M.W. Balakos, J. Catal., 157 (1995) 512.

[14] S.S.C. Chuang, M.A. Brundage, and M.W. Balakos, Appl. Catal. A., 151, (1997) 333.

[15] D.K. Kaul, and E.E. Wolf, J. Catal., 91 (1985) 216.

[16] S. Sharma, D. Boecker, G.J. Maclay, and R.D. Gonzalez, J. Catal., 110 (1988) 103.

[17] R. Krishnamurthy and S.S.C. Chuang, J. Phys. Chem., 99 (1995) 16727.

[18] S.H. Oh, G.B. Fisher, J.E. Carpenter, and D.W. Goodman, J. Catal., 100 (1986) 360.

[19] S.B. Schwartz, G.B. Fisher, and L.D. Smith, J. Phys. Chem., 92 (1988) 389.

[20] F. Solymosi and M. Pasztor, J. Phys. Chem., 89 (1985) 4789.

[21] F. Solymosi, T. Bánsági, and É. Novák, J. Catal., 112 (1988) 183.

[22] É. Novák, D. Sprinceana, and F.Solymosi, Appl. Catal. A: General 149 (1997) 89.

[23] P. Basu, D. Panayotov, and J.T. Yates, Jr., J. Am. Chem. Soc., 110 (7) (1988) 2074.

[24] W. C. Hecker, and A.T. Bell, J. Catal., 84 (1983) 200.

[25] G. Srinivas, S.S.C. Chuang and S. Debnath, J. Catal., 148 (1994) 748.

[26] S.S.C. Chuang and C.-D.Tan, Catal. Today, 35 (1997) 369.

Table 1 Dispersions of catalysts with various loadings.

	Catalysts	Active Sites (μmol)	Dispersion[a]	Chemisorption Techniques[b]	Ref.
	5 wt% Rh/SiO$_2$		0.41	• 199.18 μmol CO/g catalyst. • linear CO is the only adsorbate.	This study
a.	16.2 mg	3.23			
b.	16.2 mg	3.23			
c.	134 mg	26.69			
d.	134 mg	26.69			
	4 wt% Rh/SiO$_2$		0.62	• 61 μmol H$_2$/g catalyst. • crystallite size = 15 Å based on a cubic shape of Rh crystallites.	[25]
e.	12 mg	2.65			
f.	12 mg	2.65			
	0.5 wt% Rh/SiO$_2$		Atomic dispersion	• 31.71 μmol NO/g catalyst.	[26]
g.	101 mg	0.016			

[a] $Dispersion = \dfrac{Number\ of\ Surface\ Atoms\ on\ Support}{Total\ Number\ of\ Atoms\ on\ Support}$.

[b] All the ahemisorption studies were conducted on the reduced Rh catalysts at 303 K, with CO_{ad}/Rh = 1 and H_{ad}/Rh = 1.

Table 2
Mechanism of NO-CO reaction on Rh/SiO$_2$ and Rh single crystals.

A. Above light-off on Rh/SiO$_2$ and Rh Single Crystals

CO_g + S $\div$ CO_a

NO_g + S $\div$ NO_a

NO_a + S ' N_a + O_a

CO_a + O_a ' CO_{2g} + 2S

NO_a + N_a ' N_2O_g + S

N_a + N_a ' N_{2g} + 2S
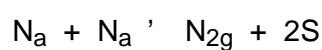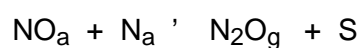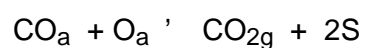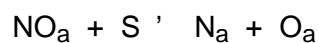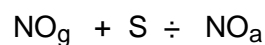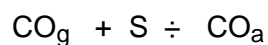
B. Below light-off on Rh/SiO$_2$

step 1 $NO_{(g)}$ + Rh^0-CO_{lin} ' Rh^0-NO^- + $CO_{(g)}$

step 2 Rh^0-NO^- + $2Rh^0$ ' $(O^{2-})2Rh^+$ + Rh^0-N

step 3 Rh^+ + NO ' Rh-NO^+

step 4   Rh-NO^+ + 2CO ' $Rh^+(CO)_2$ + $NO_{(g)}$

step 5 Rh^+ + 2CO ' $Rh^+(CO)_2$

step 6 $2Rh^+(CO)_2$ + O^{2-} ' CO_2 + $2Rh^0$-CO (linear CO) +CO

step 7 $Rh^+(CO)_2$ + $2O_{ad}$ ' $2CO_2$ + Rh^+

step 8 Rh^0-NO^- + Rh^0-N ' $2Rh^0$ + N_2O

step 9 Rh^0-N + Rh^0-N ' N_2 + $2Rh^0$
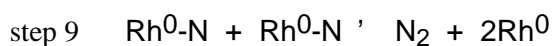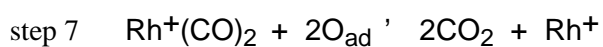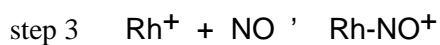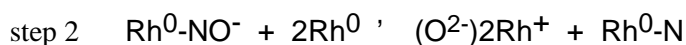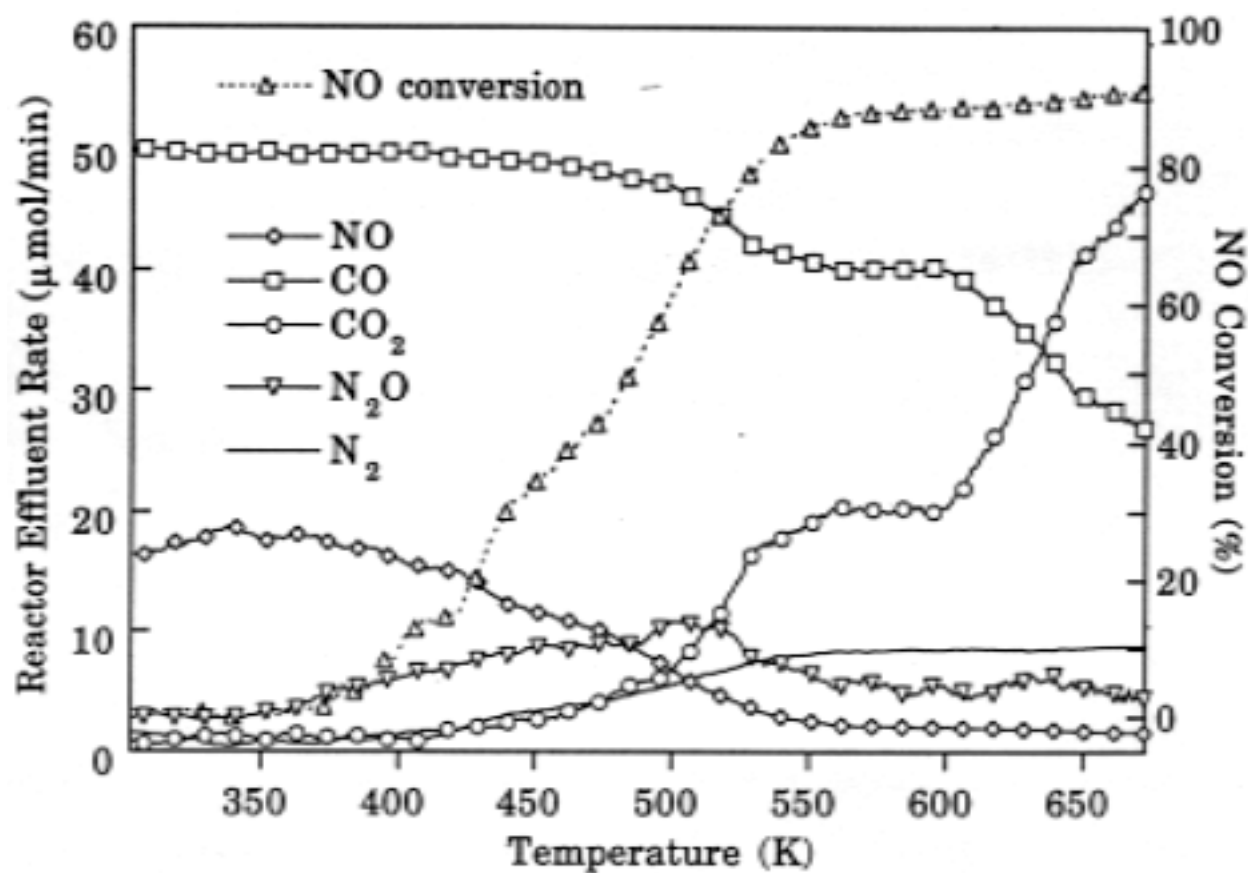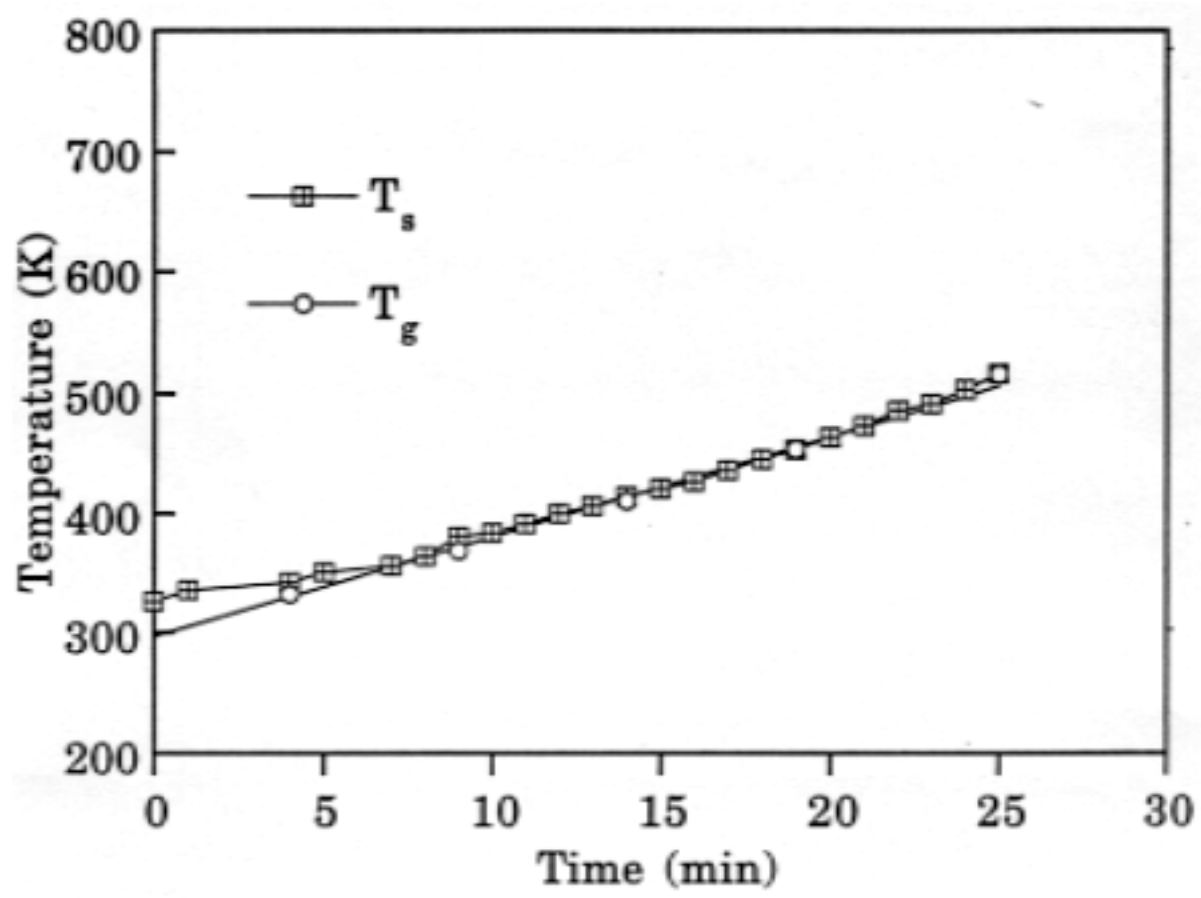
S: Rh^0 sites on rhodium single crystal
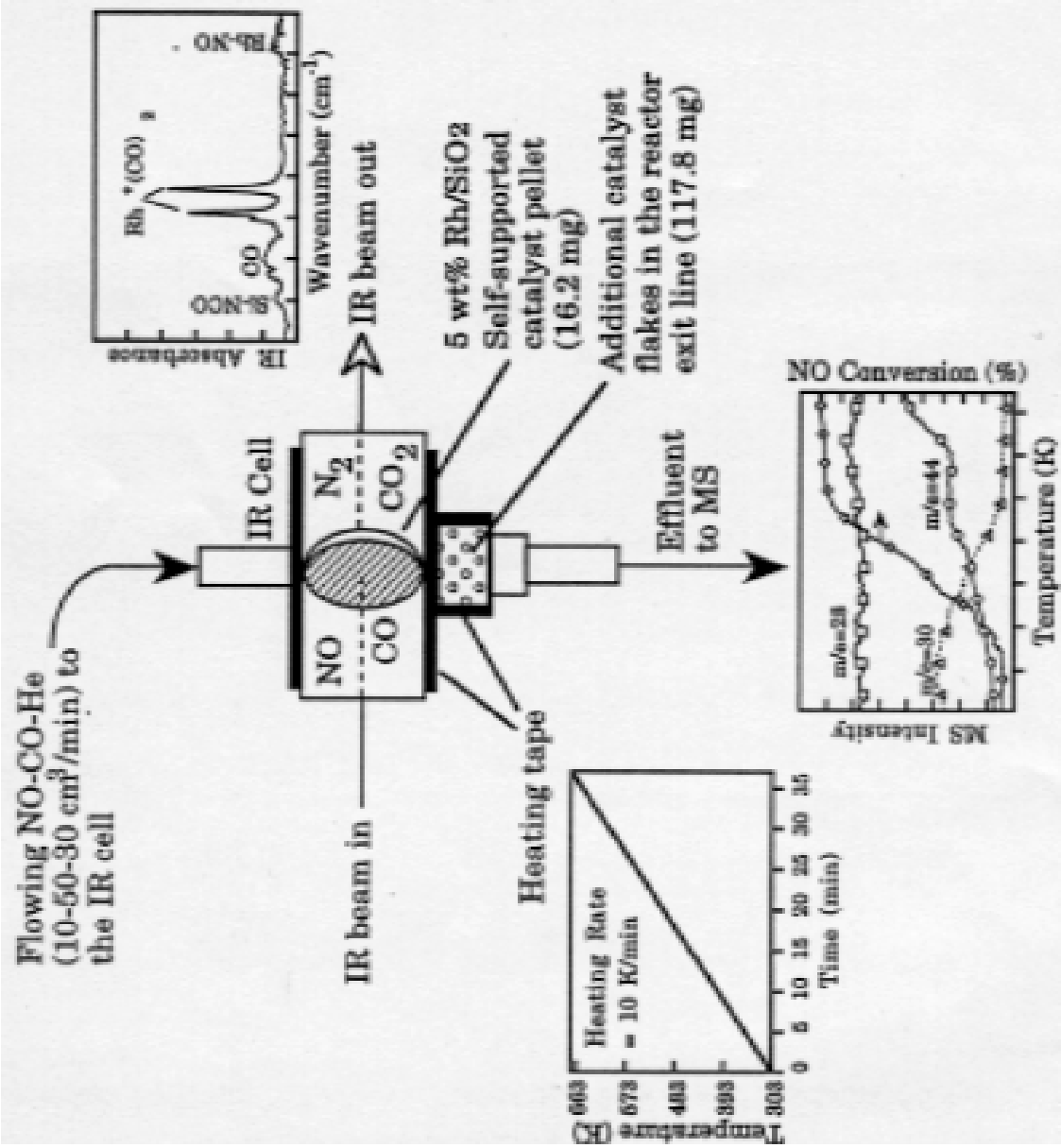
Fig. 1
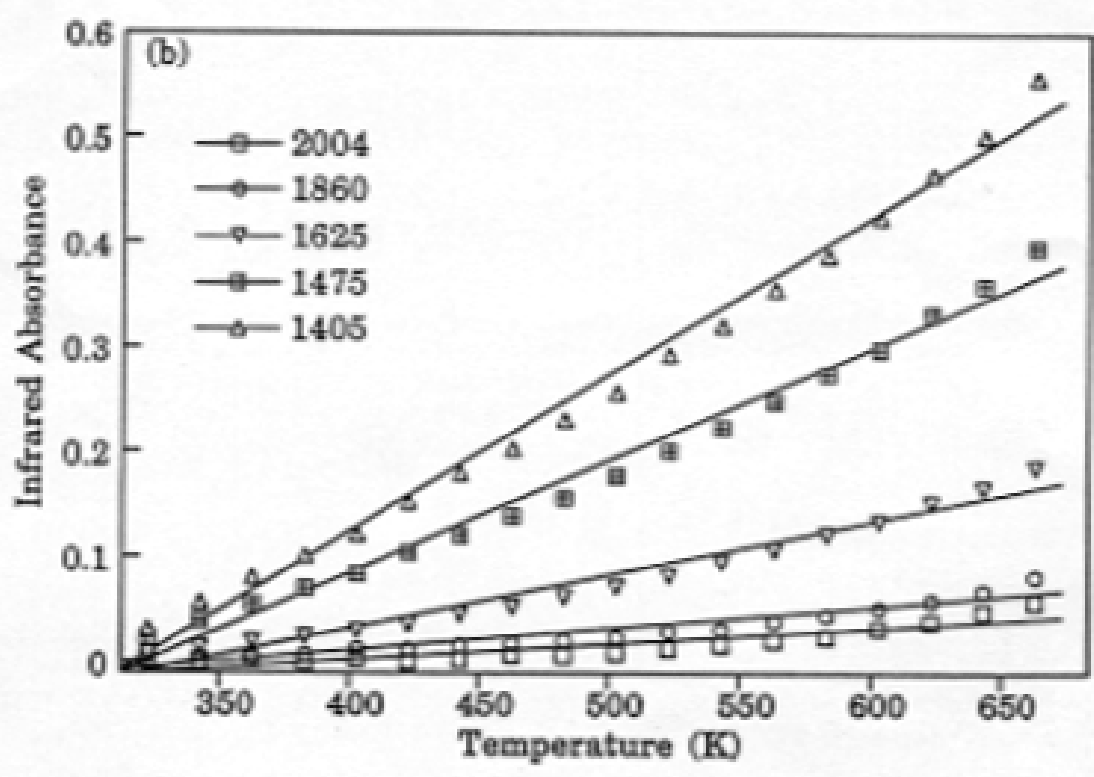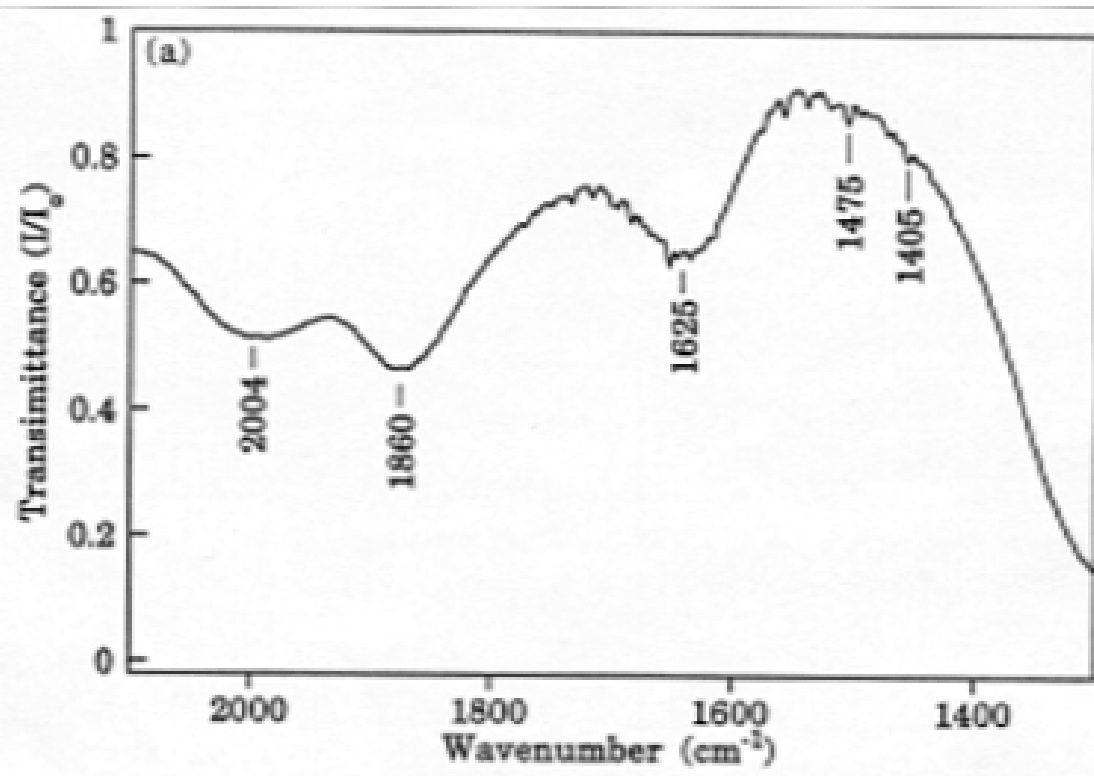
Fig 2
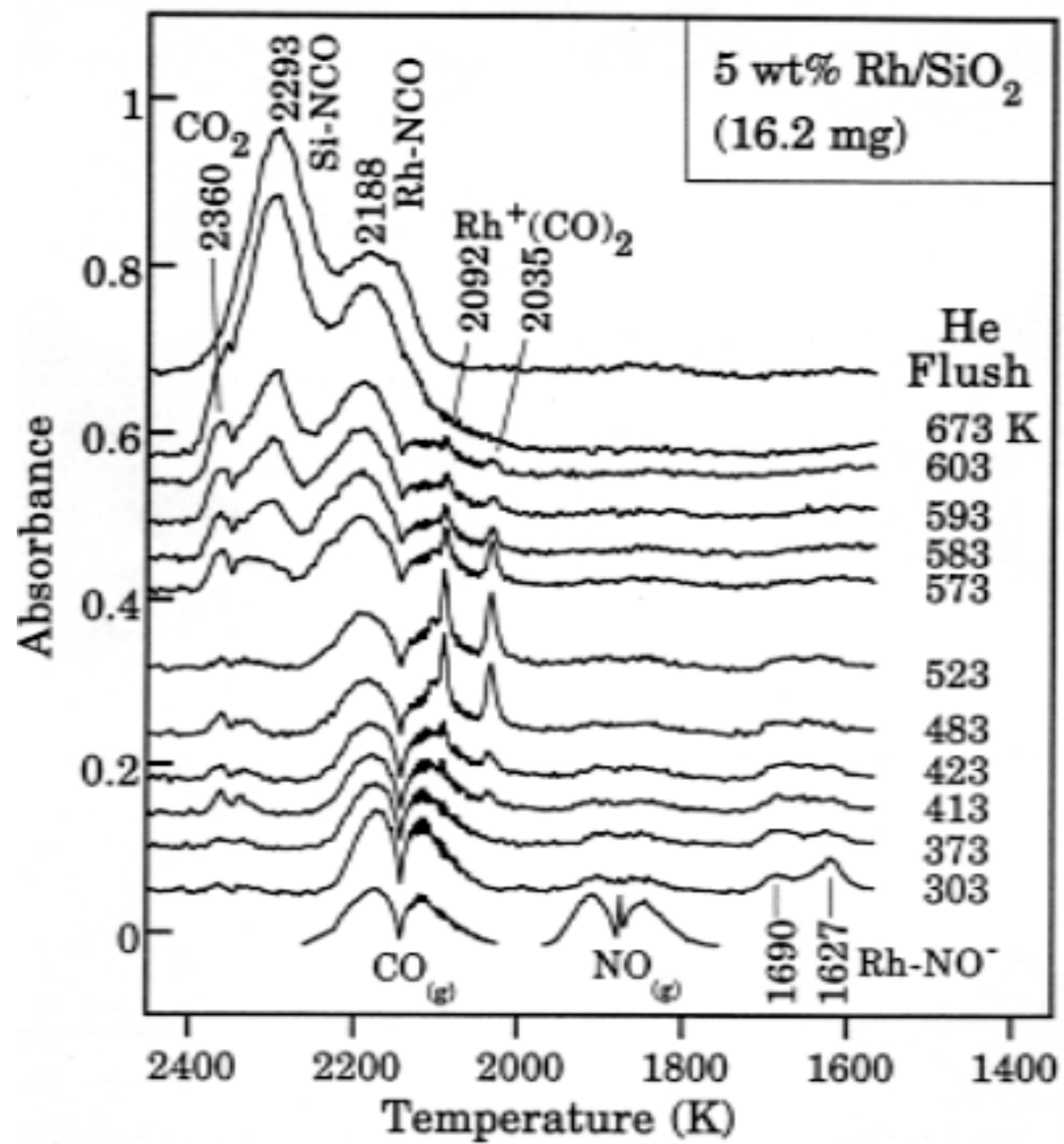
Fig 3
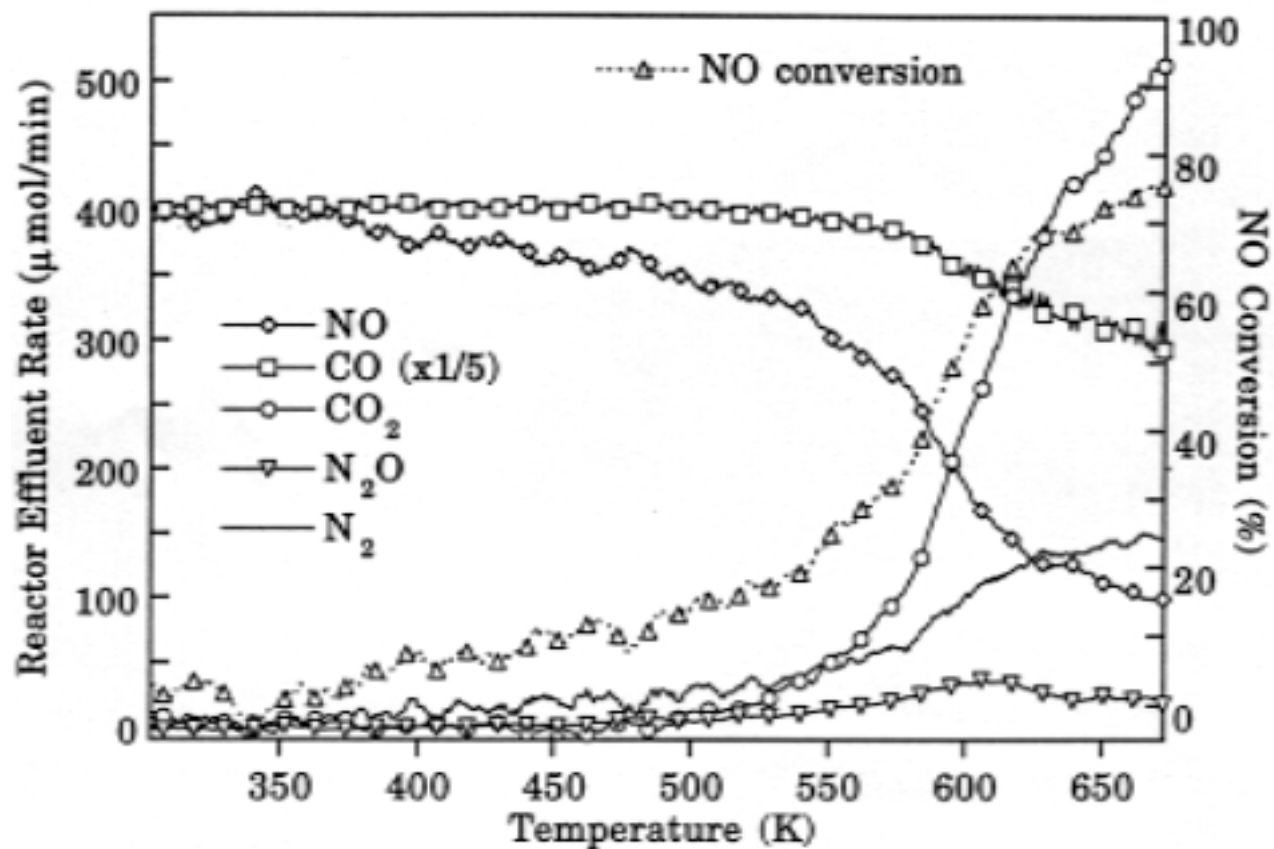
Fig. 4
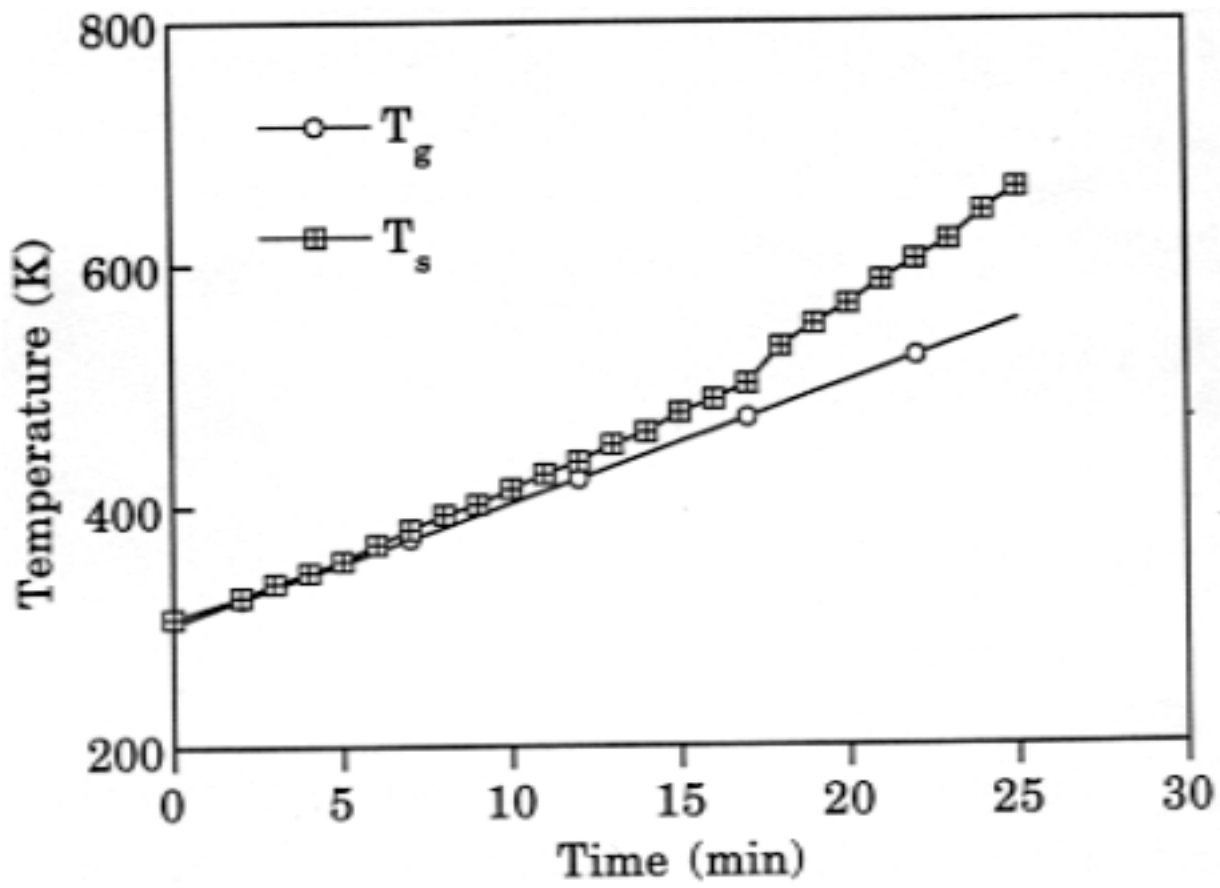
Fig 5
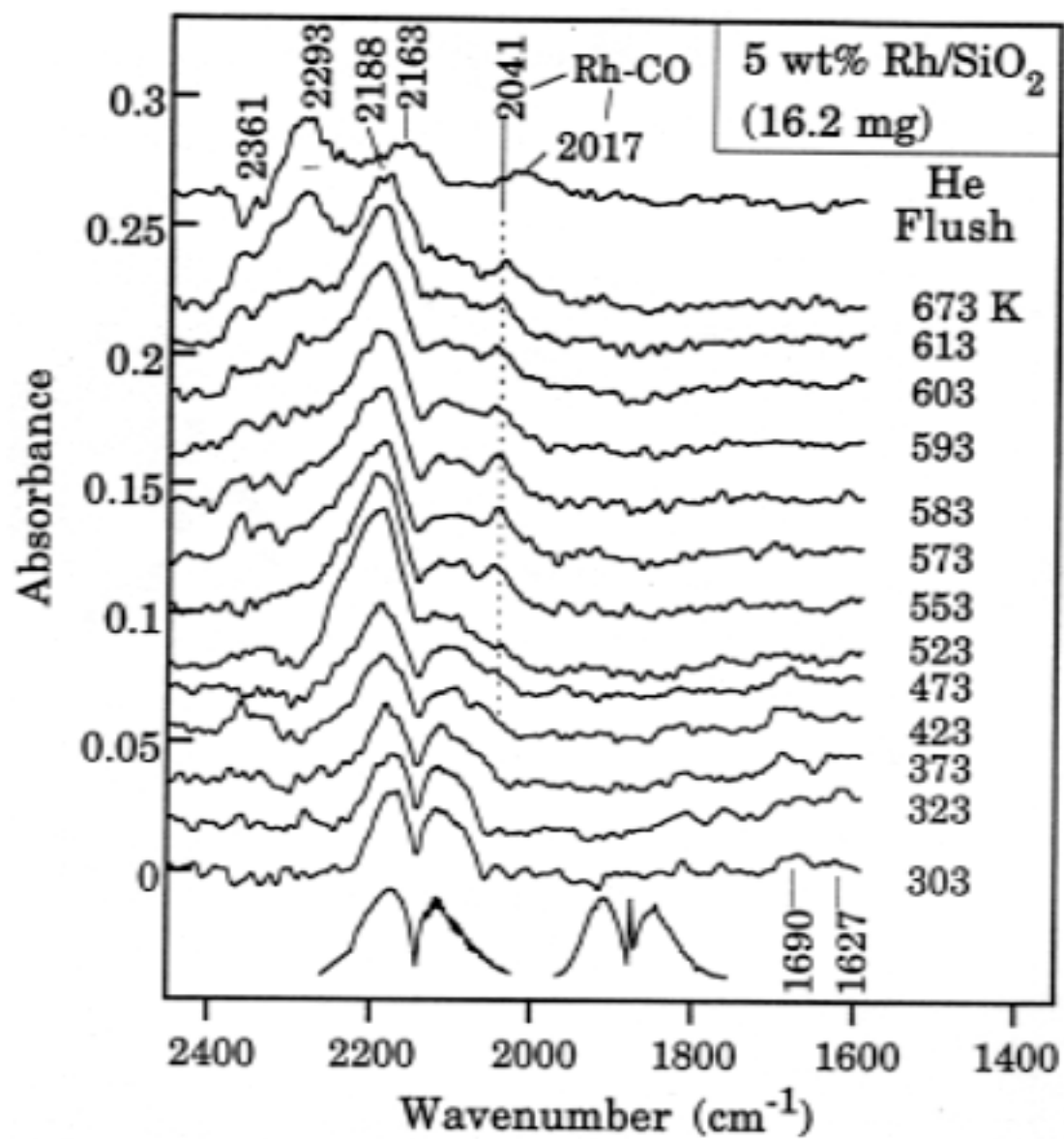
Fig 6

Fig. 7

Fig 8

Fig 9

Fig 10

Fig 11